To appear in the *International Journal of Control*
Vol. 00, No. 00, Month 20XX, 1–24

First Revision

A heat equation for freezing processes with phase change Stability analysis and applications

C.J. Backi[a,*], J.D. Bendtsen[b], J. Leth[b,**] and J.T. Gravdahl[a]

[a] *Norwegian University of Science and Technology, Department of Engineering Cybernetics, O.S. Bragstads plass 2D, 7034 Trondheim, Norway*

[b] *Aalborg University, Department of Electronic Systems, Fredrik Bajers vej 7c, 9220 Aalborg, Denmark*

(*Received 00 Month 20XX; accepted 00 Month 20XX*)

In this work the stability properties as well as possible applications of a partial differential equation (PDE) with state-dependent parameters are investigated. Among other things, the PDE describes freezing of foodstuff, and is closely related to the (Potential) Burgers' Equation. We show that for certain forms of coefficient functions, the PDE converges to a stationary solution given by (fixed) boundary conditions that make physical sense. These boundary conditions are either symmetric or asymmetric of Dirichlet type. Furthermore we present an observer design based on the PDE model for estimation of inner-domain temperatures in block-frozen fish and for monitoring freezing time. We illustrate the results with numerical simulations.

Keywords: Distributed Parameter Systems; Stability Analysis; Observer Design; Freezing Process.

1. Introduction

In order to extend the shelf life of different foodstuff, freezing has shown itself superior to many other preservation techniques. Among other reasons, freezing preserves distinct characteristics of the original product to a large extent, such as taste and nutritional value. If suitable freezing and storage methods are applied correctly, food can be stored for months or even years without significant quality degradation. Especially for rapidly spoiling food, such as fish and fish products, freezing is often essential to deliver high-quality and safe products to the consumer. Thus the physical process of freezing gets more and more attention in the scientific community and various mathematical tools describing heat transfer phenomena get applied. These tools can also be applied to other applications than freezing fish; in fact they can be applied to a whole range of physical processes where phase change occurs.

As the temperature-dynamics during freezing depend both on space and time, a good approach to model these dynamics is using distributed parameter systems (DPS), in particular partial differential equations (PDEs). As available computational power grows, the possibilities of simulating complex heat exchange processes modeled by PDEs are enhanced as well. Even if finding an explicit analytical solution to the PDE is hard or impossible, simulations can provide qualitative and quantitative results. The most common PDE for thermal problems is the famous heat equation, a parabolic PDE. The heat equation as a model for freezing problems is described in a whole range of publications, where Pham (2006b) and Pham (2006a) give an overview over how to model heat

*Corresponding author. Email: christoph.backi@ntnu.no

**J. Leth is supported by the Southern Danish Growth Forum and the European Regional Development Fund, under the project "Smart & Cool"

and mass transfer in frozen foods. A comparison between experimental and theoretical results of freezing with a simplified heat equation model is provided in Woinet, Andrieu, and Laurent (1998). Numerical results for a latent heat thermal energy storage system modeled by a diffusion equation is presented in Costa, Buddhi, and Oliva (1997), whereas Cleland, Cleland, Earle, and Byrne (1987) deliver experimental data for freezing and thawing of multi-dimensional objects modeled by finite element techniques.

An example of a PDE model describing freezing of a specific material (fish species), taking the phenomenon of *thermal arrest* caused by *latent heat of fusion* into account, was introduced in Backi and Gravdahl (2013). The parameters have to be state- (i.e. temperature)-dependent because their values change significantly not just above and below, but also around the freezing point according to the latent heat of fusion principle. In this case, the method used to model the latent heat of fusion is the so-called *apparent heat capacity method*, as introduced e.g. in Muhieddine, Canot, and March (2008). In this paper, we wish to study the stability properties of this model.

1.1 *Application-oriented aspects*

The aforementioned numerical models together with analytical models have application-oriented aspects with regard to the prediction of freezing time. Freezing time denotes the time it takes to freeze the "worst point" (the point hardest to affect - depending on geometry and freezing method) down to the safe temperature (mostly -18 °C). Analytical methods are often based on *Plank's equation*, see Plank (1941). In Pham (1985a) freezing time predictions for rectangular blocks of foodstuff are described, whereas Pham (1984) introduces an extension of Plank's equation for simple shapes. Examples for numerical modelling methods are introduced by Pham (1985b), who describes a finite-difference scheme for freezing foodstuff, and Cleland, Cleland, and Earle (1987), who present results for freezing and thawing time prediction by numerical methods.

Due to the fact that freezing time estimation is often done by simplified analytical means and prior-to-freezing-calculations, the freezing time is often overestimated. Since energy-efficiency has become a big topic in the recent past due to the finiteness of primary energy carriers as well as their impact on the climate, it is important to gain more knowledge of energy-consuming processes, such as freezing processes. In that sense a better estimation of freezing time could help terminate the freezing process even before the above mentioned analytical methods would suggest.

Again, as computational power has grown significantly in the last decades, it makes sense to introduce real time monitoring and estimation of freezing time; that is, to design state-observers which provide estimates of the non-measurable temperature field in the interior of the good's volume. With this knowledge the freezing time can be estimated. For PDE models there exist two ways to design observers, namely *early lumping* and *late lumping*. In the former approach, the spatial domain is discretized prior to the observer design (finite-dimensional), whereas in the latter, the observer is designed for the PDE itself (infinite-dimensional). An example of an *early lumping* design can be found in Kobayashi and Hitotsuya (1981), where the observer is split up into a finite- and an infinite-dimensional part. Examples of *late lumping* approaches are presented in Sallberg, Maybeck, and Oxley (2010), where an infinite-dimensional sampled data Kalman Filter is introduced and in Krstic and Smyshlyaev (2008), where transformations are used to reduce the system's complexity prior to designing the observer by backstepping methods. For an overview over different types of PDE observers see Hidayat, Babuska, Schutter, and Nunez (2011). All of the above mentioned designs have one thing in common, namely that all rely on system descriptions with constant parameters, such that transformations (e.g. gauge-transformations) can be used to obtain simplified system structures with known properties. As the system we are investigating is defined by state-dependent parameter functions, however, we cannot use the already established methods. This motivates the investigation presented in Section 4.

1.2 *Related works*

The model we consider is closely related to Burgers' equation,

$$u_t(t,x) = \epsilon u_{xx}(t,x) + u(t,x)u_x(t,x) \tag{1}$$

where subscript refers to partial derivative with respect to the argument, e.g., $u_t(t,x) \equiv \partial u(t,x)/\partial t$.

This PDE is commonly used to describe turbulent flows and is closely related to the Navier-Stokes equations. The Burgers' equation is one of the very few nonlinear partial differential equations that can be solved exactly (for a restricted set of initial functions only, and for a constant parameter ϵ). In the context of gas dynamics, Hopf (1950) and Cole (1951) independently showed that this equation can be transformed into the linear diffusion equation and solved exactly for arbitrary initial conditions (but again for constant ϵ). The study of the general properties of the Burgers' equation has motivated considerable attention due to its applications in fields as diverse as number theory, gas dynamics (Korshunova & Rozanova, 2009), heat conduction (Hills, 2006), elasticity (Sugimoto & Kakutani, 1985), special cases of transport phenomena (Hasan, Sagatun, & Foss, 2010), etc.

The stability properties of the Burgers' equation with constant and time-varying parameters have been studied previously. In Krstic (1999) stability results for both viscous and inviscid Burgers' equation are presented by defining control laws satisfying a Lyapunov analysis in the L^2-norm. Balogh and Krstic (2000) introduce H^1-stability for the Burgers' equation with nonlinear boundary feedback, whereas Krstic, Magnis, and Vazquez (2008) show results in nonlinear stabilization of shock-like unstable equilibria in the viscous Burgers' equation. Moreover, Krstic, Magnis, and Vazquez (2009) go a step further and present results for the same problem in trajectory generation, tracking and observer design.

However, as explained above, the PDE considered here represents a freezing case with phase transition. This change in phase is the reason for introducing state-dependent parameters due to the fact that the physical properties of the material to be frozen change significantly after crossing the freezing point.

This means that the parameter ϵ depends on the state variable itself, namely $\epsilon = \epsilon\left(u\left(t,x\right)\right)$, which is a more challenging case than the situations outlined above. This problem was initially introduced in Backi and Gravdahl (2013) for an application that describes the freezing of fish in a vertical plate freezer. Inspired by this problem, the present paper, among other things, investigates the stability properties of the Burgers' equation with specific functional forms of ϵ and its derivatives.

1.2.1 Parameter function $\epsilon = const.$

First of all, let us introduce the diffusion equation for a constant parameter ϵ. Let $u = u(t,x)$ be a function of two variables, time $t \in \mathbb{R}_+$ and space $x \in [0, L] \subset \mathbb{R}$. The function u must satisfy a partial differential equation of the form

$$u_t = \left[\epsilon u_x\right]_x, \quad u(0,x) = U(x), \tag{2}$$

where ϵ is a parameter and $U(x)$ denotes an initial condition. For the problem to be well posed, u must also satisfy various relevant boundary conditions. With constant ϵ, the diffusion equation (2) can be rewritten as the linear heat equation

$$u_t = \epsilon u_{xx}. \tag{3}$$

The stability properties of (2) and thus of (3) have been studied extensively in many publications, see for example Krstic and Smyshlyaev (2008). In particular, it is known that the heat equation is stable in the sense that $u(t,x) \to \bar{u}(x)$ for *any* $\epsilon > 0$, where $\bar{u}(x)$ describes the steady-state solution.

1.2.2 Parameter function $\epsilon = \epsilon(x)$

If the parameter ϵ depends on the spatial variable x, i.e. $\epsilon = \epsilon(x)$, we obtain the slightly more complicated expression for (2)

$$u_t = \epsilon_x u_x + \epsilon u_{xx}. \tag{4}$$

This may be handled by means of so-called *gauge transformations*, which eliminate the spatial dependency of $\epsilon(x)$, see e.g. Smyshlyaev and Krstic (2010). In addition, the spatial derivative of the parameter, ϵ_x, vanishes after transforming the system; hence system (4) can be transformed into system (3) for which the stability properties mentioned above are known to hold.

Similar techniques can be applied to the previously introduced Burgers' equation (1). In Heredero, Levi, and Winternitz (1999) it is shown that the standard Burgers' equation with $\epsilon = 1$,

$$u_t = u_{xx} + 2uu_x \tag{5}$$

can be transformed into the Potential Burgers' equation by using the transformation $u = v_x$, resulting in

$$v_{tx} = v_{xxx} + 2v_x v_{xx}.$$

After integrating this expression we obtain

$$v_t = v_{xx} + v_x^2$$

which represents the potential form of the Burgers' equation. After introducing the transformation $w = e^v$ the Potential Burgers' equation then boils down to the linear heat equation, as outlined above.

1.2.3 Parameter function $\epsilon = \epsilon(t)$

Finally, if the coefficient ϵ is a known function of time, Burgers' equation becomes

$$u_t = \epsilon(t)u_{xx} + uu_x. \tag{6}$$

For this case, it was shown in Sophocleous (2004) that a *time*-dependent gauge transformation exists, which transforms the nonlinear PDE into a linear one.

1.3 *Contribution*

As this paper deals with nonconstant, state-dependent parameters in the form $\epsilon = \epsilon(u(t,x))$, the earlier described transformations from Burgers' equation to linear heat equation cannot be applied. Furthermore, the system considered in Backi and Gravdahl (2013) is quite limited in actuation, meaning that only limited Dirichlet and Neumann boundary control can be applied. Strictly speaking the Dirichlet boundary condition is equal to the temperature of the cooling medium, whereas the Neumann boundary condition represents heat flux through the boundary which is proportional to the difference between the temperature at the boundary and the temperature of the cooling medium. The main contribution of the paper is to generalize the results in Backi and Gravdahl (2013) and show that under certain assumptions, the version of Burgers' equation we consider converges to a stationary solution determined by (constant) boundary conditions.

Furthermore, this paper addresses the topic of observer design for estimation of inner-domain temperatures for a freezing process. We present an observer based on an early lumping approach,

meaning that the PDE is discretized prior to the design. Due to the fact that the parameter functions depend on the state variable, established observer designs based on late lumping approaches, as introduced in Subsection 1.1, could not be applied. Therefore the observer is chosen as an Extended Kalman Filter. We show that the observer error converges to zero for the non-measurable inner-domain temperatures. These inner-domain temperatures are required in order to apply (boundary) control techniques to the PDE system, as presented in Backi and Gravdahl (2013).

1.4 *Notation*

We write f_x for the (partial) derivative of the function f with respect to x. Moreover, let $L^2([0,1])$ denote the space of real-valued, square integrable functions f defined on $[0,1]$ with finite L^2-norm; $\|f\|^2 = \int_0^1 f(x)^2 dx < \infty$. The space $H^1([0,1])$ is the subspace of $L^2([0,1])$ consisting of functions g with finite H^1-norm; $\|g\|_{H^1} = \|g\|^2 + \|g_x\|^2 < \infty$. In this paper we deal with functions $w = w(t,x)$ of time t and space x (the spatial variable). To ease notation we frequently leave out the dependency on t and/or x, e.g., $\|w(t)\|$ is the L^2-norm of the function $x \mapsto w(t)(x) = w(t,x)$.

2. Modeling

The physical process that will be modeled in this paper is the temperature distribution inside a block of foodstuff (here fish) inside a plate freezer. In Figure 1 a vertical plate freezer is displayed, whereas Figure 2 presents a typical freezing process, as it can be found on board a fishing vessel, for example. The refrigerant (liquid ammonia) is pumped through the evaporator, where it partly vaporizes while taking heat off the fish block. The separator receives the liquid-vapor mixture from the evaporator and separates phases. Then the heat added to the refrigerant will be removed in a compression-condensation-expansion cycle. This freezing process is more or less a standard vapor-compression refrigeration process with the exception that the refrigerant is not fully vaporized in the evaporator, making a separator necessary.

Figure 1. A typical vertical plate freezer (MMC Kulde AS, Ålesund, Norway)

In the case considered in the present paper and in Backi and Gravdahl (2013), a parabolic PDE is formulated in the state variable $T = T(t,x)$ representing temperature, as follows:

$$\rho(T)\, c(T)\, T_t = [\lambda(T)\, T_x]_x \tag{7}$$

subject to Dirichlet boundary conditions

$$\begin{aligned} T(t,0) &= T_0 \\ T(t,L) &= T_L \end{aligned} \tag{8}$$

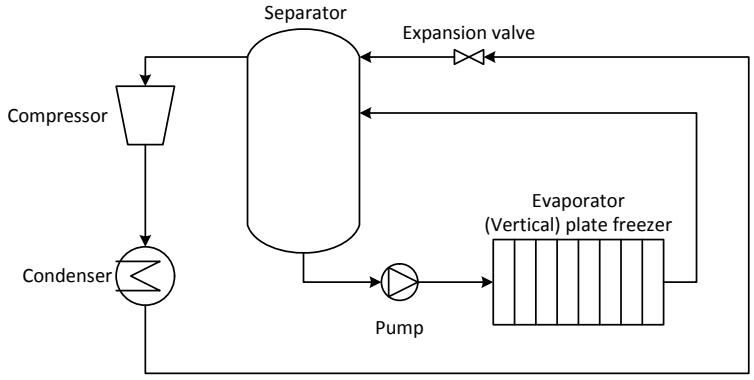

Figure 2. The freezing process

where $\rho(T)$ denotes the density, $c(T)$ indicates the specific heat capacity at constant pressure and $\lambda(T)$ describes the thermal conductivity of the medium to be frozen. Note that $\rho(T) > 0$, $c(T) > 0$ and $\lambda(T) > 0$ all depend on the temperature T. The boundary conditions T_0 and T_L are given by the refrigerant temperatures at $x = 0$ and $x = L$, respectively. Since λ depends on T, differentiation yields

$$\lambda_x(T) = \lambda_T(T) T_x$$

and thus

$$\rho(T) c(T) T_t = \lambda_T(T) T_x^2 + \lambda(T) T_{xx}. \tag{9}$$

We point out that the variation in $\rho(T)$ over T is of minor consequence and therefore we assume $\rho(T) = \rho = const$. To keep notation simple, two new parameters can be introduced as

$$k(T) = \frac{\lambda(T)}{\rho\, c(T)} \tag{10}$$

and

$$\kappa(T) = \frac{\lambda_T(T)}{\rho\, c(T)}. \tag{11}$$

This leads to a rewritten form of (9):

$$T_t = \kappa(T) T_x^2 + k(T) T_{xx}, \tag{12}$$

which is still subject to the boundary conditions defined in (8).

The heat equation (12), however, does not permit modeling for phase change phenomena, such as *thermal arrest* caused by *latent heat of fusion* (Çengel & Boles, 2004). These phenomena can be imposed to the PDE by adapting the parameter functions. In the present case this is done by applying the so called *apparent heat capacity method* as introduced e.g. in Muhieddine et al. (2008), which in principle overestimates the temperature-dependent specific heat capacity $c(T)$ around the freezing point T_F in order to slow down heat conduction.

Figure 3 displays a qualitative sketch of parameter variations in $\lambda(T)$ and $c(T)$ over T. The parameter functions were defined to approximate real parameter values sufficiently well. The transitions from c_s to c_i and from c_i to c_l are considered to be functions of the shape $c(T) = \frac{p}{T+q}$ in small neighbourhoods outside $I_{\Delta T} =]T_F - \Delta T, T_F + \Delta T[$, where p and q are constants. The model (12) holds for freezing, where both boundary conditions are strictly lower than $T_F - \Delta T$.

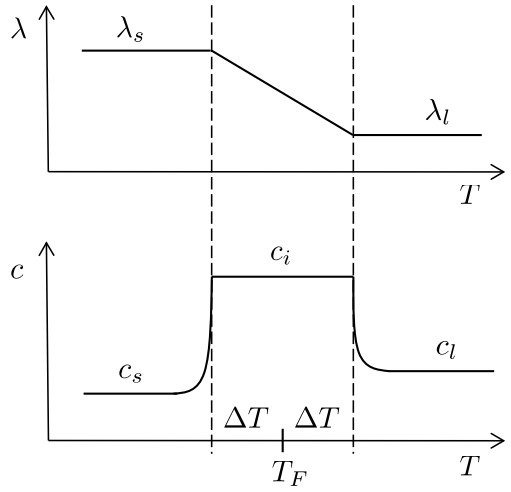

Figure 3. Qualitative sketch of parameter variations in $\lambda(T)$ and $c(T)$

The linear heat equation in the form $T_t = k\,(T)\,T_{xx}$ holds for processes where no phase change occurs, meaning all temperatures initially are and remain above or below the region $I_{\Delta T}$ around the freezing point for all t. Thus the linear heat equation is valid for both cooling and heating. In the presence of phase change, however, the additional term $\kappa\,(T)\,T_x^2$ has to be regarded as well.

As mentioned, the stability properties of the Burgers' equation have been subject to many publications. However, these results are not applicable to (12), mostly due to the fact that the effect of the non-constant parameters κ and k on the stability properties of the overall PDE are unknown. This motivates the subsequent investigation.

3. Stability Analysis

The stability investigation that is presented in this section holds for the freezing case only. This means that both boundary conditions T_0 and T_L are strictly below $T_F - \Delta T$.

3.1 *Steady state solution*

Before conducting the stability analysis of (12) we here derive an explicit formula for the steady-state solution to (12). This is done by setting $T_t = 0$, which results in

$$\kappa\,(T)\,T_x^2 + k\,(T)\,T_{xx} = 0. \tag{13}$$

For general $\kappa(T)$ and $k(T)$ the solution to the nonlinear ODE (13) can be found by evaluating the following expression:

$$C_1 x + C_2 = \int^{T(x)} \exp\Big(\int \frac{\kappa(z)}{k(z)}\,dz\Big)\,dz. \tag{14}$$

Now from physical considerations it follows that the steady state solution must be within the interval $[T_0, T_L]$ (or $[T_L, T_0]$ depending on which of T_0 and T_L is the smallest) for all values of the spatial coordinate. Also, inspired by the qualitative sketch shown in Figure 3, we henceforth state that $\kappa = 0$ outside $I_{\Delta T}$. Based on this and since we assume that the boundary conditions T_0 and T_L are strictly below $T_F - \Delta T$ we conclude that κ is zero along the steady state solution. From

(13) it then follows that the steady-state solution can be described as the solution of the ODE

$$k\left(T\right)T_{xx}=0, \tag{15}$$

which, since $k(T)>0$, has the solution

$$T(x)=C_1x+C_2. \tag{16}$$

The coefficients can be found by applying the boundary conditions to (16) leading to $C_2=T_0$ and $C_1=\frac{1}{L}(T_L-T_0)$ and thus

$$T(x)=\frac{1}{L}(T_L-T_0)x+T_0, \tag{17}$$

which represents a straight line between the two boundary values T_0 and T_L.

3.2 *Stability for asymmetric boundary conditions* $u_0 \neq u_L$

The PDE (12) is specific for the freezing application. As we intend to prove stability, however, we choose to take a more general view of the problem and to indicate this, we follow the general notation from the Introduction and change the state variable from T to u. First, we are going to investigate stability properties of (12) for asymmetric boundary conditions as defined in (8).

In general, the function u can be expressed as the sum of a transient part $w(t,x)$ and a stationary part $\bar{u}(x)$, i.e. $u(t,x)=w(t,x)+\bar{u}(x)$. Here, $\bar{u}(x)$ is a function of x due to the asymmetric boundary conditions, and as we have shown above, $\bar{u}(x)$ takes a function of the form $\bar{u}(x)=Sx+R$, where S and R are constants. Furthermore, we normalize the spatial coordinate to belong to $[0,1]$. With these conventions, we study the following equivalent form of (12):

$$\begin{aligned} w_t =&\frac{\kappa}{L^2}(w_x+S)^2+\frac{k}{L^2}w_{xx}\\ =&\frac{\kappa}{L^2}(w_x^2+S^2+2Sw_x)+\frac{k}{L^2}w_{xx} \end{aligned} \tag{18a}$$

with boundary conditions

$$w(t,0)=w(t,1)=0. \tag{18b}$$

Remark 1: We must point out that our focus lies on continuously differentiable solutions with finite H^1-norm only. From a stringent mathematical point of view the question of existence of such solutions is a crucial aspect, however, we will not approach that here. For the (related) Stefan problem we refer to Prüss, Saal, and Simonett (2007), who provide a treatment of the existence of solutions for that case. Nevertheless, our application studies indicate that at least some solutions of this form exist.

Lemma 1: *Let w satisfy* (18a)–(18b). *Suppose that there exist constants $\beta>\alpha>0$ such that*

$\alpha \leq k \leq \beta$. *If*

$$(\kappa + k_u)^2 < 2\left(\kappa k_u - k_{uu}k + k_u^2\right) \tag{19a}$$

$$k_{uu}k < k_u^2 + \kappa k_u \tag{19b}$$

$$w > 0 \ \forall u \in \ I_{\Delta u} \tag{19c}$$

$$\kappa k_u \geq 0 \tag{19d}$$

$$k_{uu} \leq 0 \ \forall u \in \ I_{\Delta u} \tag{19e}$$

$$\kappa < 0 \ \forall u \in \ I_{\Delta u} \tag{19f}$$

$$\kappa \equiv 0 \ \forall u \notin \ I_{\Delta u} \tag{19g}$$

then $\|w(t)\| \to 0$ *as* $t \to \infty$.

The details of the assumptions in Lemma 1 will be discussed at the end of this subsection.

Proof. Define the Lyapunov candidate V by

$$V = \int_0^1 \frac{1}{k} w^2 \, dx \tag{20}$$

and note that

$$V \geq \frac{1}{\beta}\|w(t)\|^2 \tag{21}$$

since $k \leq \beta$ by assumption.

Differentiating (20) with respect to time leads to

$$\begin{aligned}\dot{V} =& \int_0^1 \frac{2}{k} w w_t - \frac{k_u}{k^2} w^2 w_t \, dx \\ =& \frac{1}{L^2} \int_0^1 \Big(\frac{2\kappa}{k} \, w w_x^2 + \frac{2\kappa}{k} \, w S^2 + \frac{4\kappa}{k} \, w S w_x + 2 \, w w_{xx} \\ & - \frac{\kappa k_u}{k^2} \, w^2 w_x^2 - \frac{\kappa k_u}{k^2} \, w^2 S^2 - \frac{2\kappa k_u}{k^2} \, w^2 S w_x - \frac{k_u}{k} \, w^2 w_{xx} \Big) \, dx.\end{aligned} \tag{22}$$

Integrating the terms $w w_{xx}$ and $\frac{k_u}{k} w^2 w_{xx}$ by parts yields

$$\int_0^1 w w_{xx} \, dx = \Big[w w_x \Big]_0^1 - \int_0^1 w_x^2 \, dx \tag{23}$$

$$\int_0^1 \frac{k_u}{k} w^2 w_{xx} \, dx = \Big[\frac{k_u}{k} w^2 w_x \Big]_0^1 - 2 \int_0^1 \frac{k_u}{k} w w_x^2 \, dx - \int_0^1 \frac{k_{uu}k - k_u^2}{k^2} w^2 w_x^2 \, dx. \tag{24}$$

with $\Big[w w_x \Big]_0^1 = 0$ and $\Big[\frac{k_u}{k} w^2 w_x \Big]_0^1 = 0$ due to (18b). Then, after inserting (23) and (24) into (22)

and collecting terms the following expression is obtained

$$\dot{V} = \frac{1}{L^2}\int_0^1 \frac{1}{k}\Big[Aw_x^2 + Bw_x + C\Big]\, dx \tag{25}$$

where we have used the shorthand

$$A = -w^2\frac{1}{k}(\kappa k_u - k_{uu}k + k_u^2) + w(2\kappa + 2k_u) - 2k \tag{26a}$$

$$B = w^2\frac{1}{k}(-2\kappa k_u S) + w(4\kappa S) \tag{26b}$$

$$C = w^2\frac{1}{k}(-\kappa k_u S^2) + w(2\kappa S^2). \tag{26c}$$

Note that $A < 0$, since the coefficients

$$a = -\frac{1}{k}(\kappa k_u - k_{uu}k + k_u^2) \tag{27a}$$

$$b = 2\kappa + 2k_u \tag{27b}$$

$$c = -2k \tag{27c}$$

of the parabola $aw^2 + bw + c$ defined by (26a) fulfill $a < 0$ and $b^2 - 4ac < 0$, by (19a)–(19b).

The rest of the proof consists of the following two observations outside and inside $I_{\Delta T}$, respectively.

The first observation is based upon the fact that outside $I_{\Delta T}$ both $B = 0$ and $C = 0$ due to (19g). Hence, for this case, we can bound (25) using that $\frac{1}{\beta} \leq \frac{1}{k}$ followed by applying *Poincaré's Inequality* (Krstic & Smyshlyaev, 2008, Lemma 2.1), leading to

$$\dot{V} \leq \frac{K_1}{L^2\beta}\|w_x\|^2 \leq \frac{K_1}{4L^2\beta}\|w\|^2 \tag{28}$$

with $K_1 = \max(A) < 0$.

For the second observation we note that the inequality $B^2 - 4AC < 0$ is satisfied inside $I_{\Delta T}$, as can be seen as follows. Using (26) the inequality $B^2 - 4AC < 0$ is equivalent to the following quartic inequality

$$\frac{w^4}{k^4}\Big(4\kappa k_u S^2(k_{uu}k - k_u^2)\Big) + \frac{w^3}{k^3}\Big(-8\kappa S^2(k_{uu}k - 2k_u^2)\Big) + \frac{w^2}{k^2}\Big(-24\kappa k_u S^2\Big) + \frac{w}{k}\Big(16\kappa S^2\Big) < 0. \tag{29}$$

Let

$$\psi(w) = a_4w^4 + a_3w^3 + a_2w^2 + a_1w$$

denote the 4th order polynomial defined by the left hand side of (29) and note that $a_i < 0,\ i = 1, 2, 3, 4$ inside $I_{\Delta T}$ by the assumptions (19d)–(19f). Let $\phi(w)$ denote the 3rd order polynomial defined by $\psi(w) = w\phi(w)$. Then (29) holds inside $I_{\Delta T}$ iff $\phi(w) < 0$ for $w > 0$ (assumption (19c)). Since both, $a_4 < 0$ and $a_1 < 0$ inside $I_{\Delta T}$, it is enough to show that the roots of $\phi(w)$ all are negative or complex, which follows from the fact that inside $I_{\Delta T}$ we have $a_4 < 0$, $\phi_w(0) = a_2 < 0$

and $\phi_{ww}(0) = a_3 < 0$. Hence, as long as we are inside $I_{\Delta T}$ there exists a constant $K_2 < 0$ such that

$$\dot{V} \leq \frac{K_2}{L^2\beta}\|w_x\|^2 \leq \frac{K_2}{4L^2\beta}\|w\|^2 \tag{30}$$

By letting $\bar{K} = \max\{K_1, K_2\}$, inequalities (28) and (30) now yield

$$\dot{V} \leq \frac{1}{4L^2\beta}\bar{K}\|w\|^2 \tag{31}$$

which together with (20) and Henry (1981, Theorem 4.1.4) proves the lemma. □

We now extend Lemma 1 to the H^1-case.

Lemma 2: *Suppose that the assumptions of Lemma 1 hold true. If moreover*

$$\kappa_u \leq 0 \tag{32a}$$

$$w_x(t,1)w_{xx}(t,1) - w_x(t,0)w_{xx}(t,0) \leq 0 \tag{32b}$$

$$\kappa S\Big(w_x^2(t,1) - w_x^2(t,0)\Big) \leq 0 \tag{32c}$$

$$\kappa\Big(w_x^3(t,1) - w_x^3(t,0)\Big) \leq 0 \tag{32d}$$

then the origin is globally asymptotically stable (wrt $\|\cdot\|_{H^1}$). In particular $\|w(t)\|_{H^1} \to 0$ as $t \to \infty$.

Proof. Define the Lyapunov candidate Λ by

$$\Lambda = V_1 + V = \frac{1}{2}\int_0^1 w_x^2\, dx + V \tag{33}$$

where V denotes the Lyapunov function defined by (20). The time derivative of V_1 is

$$\dot{V}_1 = \int_0^1 w_x w_{tx}\, dx. \tag{34}$$

To obtain an expression for w_{tx} in terms of spatial derivatives of w only, the derivative of (18) with respect to x is calculated and one obtains

$$w_{tx} = \frac{1}{L^2}\Big(\kappa_u w_x^3 + 2\kappa_u S w_x^2 + \kappa_u S^2 w_x + 2\kappa w_x w_{xx} + 2\kappa S w_{xx} + k_u w_x w_{xx} + k w_{xxx}\Big). \tag{35}$$

Combining (35) and (34) and collecting terms gives

$$\dot{V}_1 = \frac{1}{L^2}\int_0^1 \Big(\kappa_u w_x^4 + 2\kappa_u S w_x^3 + \kappa_u S^2 w_x^2 + 2\kappa w_x^2 w_{xx} + 2\kappa S w_x w_{xx} + k_u w_x^2 w_{xx} + k w_x w_{xxx}\Big)\, dx. \tag{36}$$

Integrating the terms kw_xw_{xxx} and κw_xw_{xx} by parts yields

$$\int_0^1 kw_xw_{xxx}\,dx = \Big[kw_xw_{xx}\Big]_0^1 - \int_0^1 kw_{xx}^2\,dx - \int_0^1 k_uw_x^2w_{xx}\,dx \tag{37}$$

$$\begin{aligned}\int_0^1 \kappa w_xw_{xx}\,dx &= \Big[\kappa w_x^2\Big]_0^1 - \int_0^1 \kappa w_xw_{xx}\,dx - \int_0^1 \kappa_u w_x^3\,dx \\ &= \Big[\frac{\kappa}{2}w_x^2\Big]_0^1 - \int_0^1 \frac{\kappa_u}{2}w_x^3\,dx.\end{aligned} \tag{38}$$

Putting (37) and (38) into (36) one obtains

$$\dot{V}_1 = \frac{1}{L^2}\int_0^1 \Big(\kappa_u w_x^4 + \kappa_u S w_x^3 + \kappa_u S^2 w_x^2 + 2\kappa w_x^2 w_{xx} - kw_{xx}^2\Big)\,dx + \frac{1}{L^2}\Big[kw_xw_{xx} + \kappa S w_x^2\Big]_0^1. \tag{39}$$

Furthermore, integrating the expression $\kappa w_x^2w_{xx}$ by parts gives

$$\begin{aligned}\int_0^1 \kappa w_x^2w_{xx}\,dx &= \Big[\kappa w_x^3\Big]_0^1 - \int_0^1 2\kappa w_x^2w_{xx}\,dx - \int_0^1 \kappa_u w_x^4\,dx \\ &= \Big[\frac{1}{3}\kappa w_x^3\Big]_0^1 - \int_0^1 \frac{1}{3}\kappa_u w_x^4\,dx.\end{aligned} \tag{40}$$

After substituting (40) into (39) we receive

$$\dot{V}_1 = \frac{1}{L^2}\int_0^1 \Big(\frac{\kappa_u}{3}w_x^4 + \kappa_u S w_x^3 + \kappa_u S^2 w_x^2 - kw_{xx}^2\Big)\,dx + \frac{1}{L^2}\Big[kw_xw_{xx} + \kappa S w_x^2 + \frac{2\kappa}{3}w_x^3\Big]_0^1. \tag{41}$$

Now we need to have a closer look at the quartic equation $\theta(w_x) = dw_x^4 + ew_x^3 + fw_x^2$ with the shorthand

$$d = \frac{\kappa_u}{3}, \quad e = \kappa_u S, \quad f = \kappa_u S^2,$$

which can be rewritten as $w_x^2\gamma(w_x)$. For the quadratic equation $\gamma(w_x)$ we must impose that it is less than zero for all w_x and thus it must hold that $d < 0$ and $e^2 - 4df \leq 0$. If now (32a) holds, we see that $\gamma(w_x) < 0$ for all w_x and therefore $\theta(w_x) < 0$. If furthermore (32b)–(32d) hold, we can infer that

$$\dot{V}_1 \leq -\frac{1}{L^2}\int_0^1 kw_{xx}^2\,dx \leq -\frac{\alpha}{L^2}\int_0^1 w_{xx}^2\,dx. \tag{42}$$

Thus by putting (31) and (42) into the time-derivative of (33), using Krstic and Smyshlyaev (2008, Lemma 2.1) (*Poincaré's Inequality*) and recalling that $\bar{K} < 0$, we receive

$$\begin{aligned}\dot{\Lambda} &\leq -\frac{\alpha}{L^2}\int_0^1 w_{xx}^2\,dx + \frac{\bar{K}}{L^2\beta}\int_0^1 w_x^2\,dx \leq \frac{\bar{K}}{L^2\beta}\int_0^1 w_x^2\,dx \\ &\leq \frac{\bar{K}}{2L^2\beta}\int_0^1 w_x^2\,dx + \frac{\bar{K}}{2L^2\beta}\int_0^1 w_x^2\,dx \\ &\leq \frac{\bar{K}}{8L^2\beta}\int_0^1 w^2\,dx + \frac{\bar{K}}{2L^2\beta}\int_0^1 w_x^2\,dx \\ &\leq \frac{\bar{K}}{8L^2\beta}\|w(t)\|_{H^1},\end{aligned} \tag{43}$$

which, together with (33) and Henry (1981, Theorem 4.1.4) proves the lemma. □

Together with *Agmon's Inequality* (Krstic & Smyshlyaev, 2008, Lemma 2.4), Lemma 2 now immediately implies the following main result of the paper.

Theorem 1: *Let w satisfy* (18a)–(18b). *Suppose that the assumptions of Lemma 2 are satisfied. Then $w(t,x) \to 0$ as $t \to \infty$, hence $u(t,x) \to \bar{u}(x)$ as $t \to \infty$.*

3.2.1 Discussion of the assumptions in Lemma 1 and Lemma 2

The assumptions in Lemma 1 and Lemma 2 impose limitations on the parameter functions $k(u)$ and $\kappa(u)$ and their respective derivatives with respect to u. In Lemma 1 assumptions (19d)–(19g) are satisfied due to the definition of the parameter functions in Figure 3. Assumption (19c) holds true due to the fact that the boundary conditions are chosen constant below the region $I_{\Delta u}$ and the definition of w in the beginning of this subsection. Assumptions (19a)–(19b) have to be imposed to the problem and are valid, also due to the definition of the parameter functions.

In Lemma 2 assumption (32a) is satisfied by the definition of the parameter functions, again see Figure 3. Assumptions (32b)–(32d) define conditions for the temperature change with respect to the spatial domain and its derivative, both evaluated at the respective boundaries.

3.3 *Stability for symmetric boundary conditions $u_0 = u_L$*

In the case of symmetric boundary conditions, which represents a special case of the above investigation, one can use the same fundamentals of the previously conducted proofs. Note that the boundary condition in (18b) will stay the same, but the boundary condition in (8) in terms of u as state variable becomes

$$u(t,0) = u(t,L) = u_B.$$

In fact, to prove stability for symmetric boundary conditions, we can use the same Lyapunov functions and are thus able to state almost identical versions of Lemma 1 and Lemma 2, but with a reduced amount of assumptions on the parameter functions. In Lemma 1 particularly, assumptions (19c)–(19g) can be removed. This is due to the fact that all terms including S disappear, as $S = 0$. This is valid due to the fact that the steady state solution is now represented by a constant straight

line between the two boundary values

$$u(x) = u_B = const.$$

That this is actually valid can be shown be calculation using the results presented in Subsection 3.1. Therefore, (25) can be rewritten in a reduced form

$$\dot{V} = \frac{1}{L^2} \int_0^1 \frac{1}{k} A w_x^2 \, dx \tag{44}$$

with A defined in (26a) and thus only (19a)–(19b) are required to hold in order for $\|w(t)\| \to 0$ as $t \to \infty$. In (41) the terms containing S can be removed due to the same argument as used above and thus it can be changed into

$$\dot{V}_1 = \frac{1}{L^2} \int_0^1 \frac{\kappa_u}{3} w_x^4 - k w_{xx}^2 \, dx + \frac{1}{L^2} \Big[k w_x w_{xx} + \frac{2\kappa}{3} w_x^3 \Big]_0^1.$$

We can directly see that now only assumptions (32a)–(32b) and (32d) have to be fulfilled in order for $\|w(t)\|_{H^1} \to 0$ as $t \to \infty$. The argumentation in Theorem 1 is untouched by these changes, as the reduced versions of both, Lemma 1 and Lemma 2, hold for the case with symmetric boundary conditions. However, we must point out that $w(t,x) \to 0$ as $t \to \infty$, but now $u(t,x) \to u_B$ as $t \to \infty$, meaning that $u(t,x)$ now tends to the steady state value $u(x) = u_B$, which is constant over the whole spatial domain.

4. Observer

In this section we want to provide a possible application for the model (12), namely an observer design with the aim to estimate the temperature distribution throughout a block of foodstuff. This can be used to monitor freezing time.

4.1 *Observer model*

The model for the observer design is based upon (12), but in a 2-dimensional formulation.

The model describes thus the temperature distribution $T = T(t,x,y)$ throughout a block of fish that is frozen inside a vertical plate freezer

$$\begin{aligned} \rho(T)c(T)T_t &= \big(\lambda(T)T_x\big)_x + \big(\lambda(T)T_y\big)_y \\ &= \lambda_T(T)\big(T_x^2 + T_y^2\big) + \lambda(T)\big(T_{xx} + T_{yy}\big) \end{aligned} \tag{45}$$

where $\rho(T)$, $c(T)$ and $\lambda(T)$ have been introduced in Section 2. Rewritten, (45) becomes

$$T_t = \kappa(T)\big(T_x^2 + T_y^2\big) + k(T)\big(T_{xx} + T_{yy}\big) \tag{46}$$

where $k(T)$ and $\kappa(T)$ have been defined in (10) and (11), respectively.

The effects of the freezing medium (vaporizing liquid ammonia) at $x = 0$ and $x = L$ as well as of exposure to air ($y = 0$) are modeled by Dirichlet boundary conditions, whereas presumed perfect insulation at the bottom of the fish block ($y = h$) is modeled by Neumann boundary conditions.

Note that the boundary inputs at $x = 0$ and $x = L$ are not actively controlled. As an introduction to the upcoming subsections we illustrate in Figure 4 how the spatial domain is discretized and furthermore which of the states are measurable (orange) and which are not (blue). In addition Figure 4 shows how the boundary conditions are chosen and the way they act on the system.

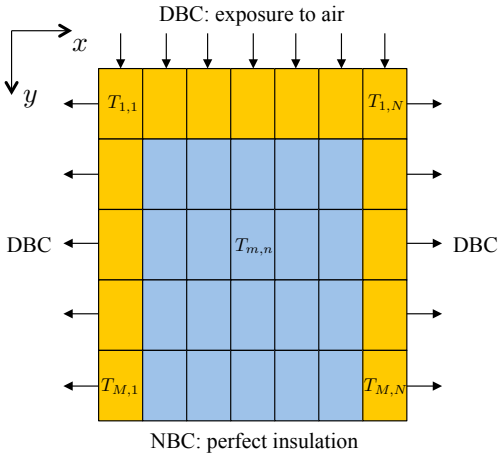

Figure 4. DBC denotes Dirichlet boundary conditions and NBC denotes Neumann boundary conditions

4.1.1 Discretization

Discretization is performed by means of finite difference methods for the spatial derivatives only. This corresponds with an *early lumping* approach and will lead to an approximation of the PDE by a set of coupled ODEs. For discretization it is necessary to use uneven discretization numbers N and M in x- and y-direction, in order to be able to define central layers for both spatial domains.

The terms T_x and T_y will both be approximated by first order forward and central difference methods. It is important to mention that, in this case, the discretization direction is not consistent with positive x- and y-directions. This means that discretization is performed from the left/right and from the bottom/top boundaries towards the central layers of the spatial domain using a first order forward difference approach, whereas a first order central difference approach is used at the very center of the spatial domain, both regarding x- and y-directions. The reason for this is that the boundary conditions at $x = 0$ and $x = L$ must be imposed to the discretized equations with the same sign (here positive), which will not be the case with a consistent discretization direction.

The following discretizations are defined for fixed y- and x-positions, respectively

$$T_x = \begin{cases} \frac{T_{m,n-1} - T_{m,n}}{\Delta x}, & \text{if } n < \frac{N+1}{2} \\ \frac{T_{m,n+1} - 2T_{m,n} + T_{m,n-1}}{2\Delta x}, & \text{if } n = \frac{N+1}{2} \\ \frac{T_{m,n+1} - T_{m,n}}{\Delta x}, & \text{if } n > \frac{N+1}{2}, \end{cases} \tag{47}$$

$$T_y = \begin{cases} \frac{T_{m-1,n} - T_{m,n}}{\Delta y}, & \text{if } m < \frac{M+1}{2} \\ \frac{T_{m+1,n} - 2T_{m,n} + T_{m-1,n}}{2\Delta y}, & \text{if } m = \frac{M+1}{2} \\ \frac{T_{m+1,n} - T_{m,n}}{\Delta y}, & \text{if } m > \frac{M+1}{2}. \end{cases} \tag{48}$$

Note that the terms for $n = \frac{N+1}{2}$ and $m = \frac{M+1}{2}$ in (47) and (48) are computed by using central

differences instead of forward differences

$$\frac{T_{m,n+1}-2T_{m,n}+T_{m,n-1}}{2\Delta x}=\frac{1}{2}\frac{T_{m,n-1}-T_{m,n}}{\Delta x}+\frac{1}{2}\frac{T_{m,n+1}-T_{m,n}}{\Delta x},$$
$$\frac{T_{m+1,n}-2T_{m,n}+T_{m-1,n}}{2\Delta y}=\frac{1}{2}\frac{T_{m-1,n}-T_{m,n}}{\Delta y}+\frac{1}{2}\frac{T_{m+1,n}-T_{m,n}}{\Delta y}.$$

The approximations for the terms T_{xx} and T_{yy} are obtained by using a second order central difference method. This approach can be applied by following a consistent discretization direction, due to the fact that the boundary conditions enter the discretized equations with the same sign. As a result the following equations hold for fixed y- and x-positions, respectively

$$T_{xx}=\frac{T_{m,n+1}-2T_{m,n}+T_{m,n-1}}{\Delta x^2}, \tag{49}$$
$$T_{yy}=\frac{T_{m+1,n}-2T_{m,n}+T_{m-1,n}}{\Delta y^2}. \tag{50}$$

The discrete expressions (47), (48), (49) and (50) are defined for $1 \leq n \leq N$ and $1 \leq m \leq M$, where the values at $T_{m,0}$, $T_{m,N+1}$, $T_{0,n}$ and $T_{M+1,n}$ represent the fictional states where the boundary conditions enter the equations. The discretization step sizes are $\Delta x = \frac{L}{N}$ and $\Delta y = \frac{h}{M}$, where h defines the height of the fish block. This discretization procedure will lead to $N \times M$ coupled ordinary differential equations (ODEs). For $1 \leq n < \frac{N+1}{2}$ and $1 \leq m < \frac{M+1}{2}$, a general description of this ODE has the form

$$\begin{aligned}\dot{T}_{m,n} =&\kappa(T_{m,n})\Big[\Big(\frac{T_{m,n-1}-T_{m,n}}{\Delta x}\Big)^2+\Big(\frac{T_{m-1,n}-T_{m,n}}{\Delta y}\Big)^2\Big]\\ &+k(T_{m,n})\Big[\frac{T_{m,n+1}-2T_{m,n}+T_{m,n-1}}{\Delta x^2}+\frac{T_{m+1,n}-2T_{m,n}+T_{m-1,n}}{\Delta y^2}\Big].\end{aligned} \tag{51}$$

4.1.2 Boundary conditions

As mentioned before, Dirichlet boundary conditions are imposed on the system at $T_{m,0}$, $T_{m,N+1}$ and $T_{0,n}$. We point out that these boundary conditions are assumed constant and can therefore be defined as $T_{m,0} = T_{m,N+1} = T_{Ammonia}$ for all m and $T_{0,n} = T_{Air}$ for all n. Furthermore, perfect insulation at the bottom of the fish block is defined by Neumann boundary conditions at $T_{M+1,n}$, leading to the expression $T_{M+1,n} - T_{M,n} = 0$ for all n.

4.2 *Observer*

The observer is designed to estimate the unmeasurable states inside the spatial domain of the fish block. For this system, inner-domain measurements are difficult to set up and thus not practical. The estimation of the unmeasurable states is important to predict when the desired temperature is reached inside the inner layers of the spatial domain. Thus it can replace simpler, approximative freezing time prediction methods.

A first choice for a practical observer design is often a Kalman Filter based design. Due to the fact that a Kalman Filter is a well-established observer in engineering practice, it is often used as a benchmark in order to compare other observer designs with regard to performance. The Kalman Filter has certain robustness properties which are based on the fact that modeling and measurement errors are introduced to the system model by adding up white Gaussian noise signals v and z to the state derivatives and the outputs, respectively. Here we will investigate the possibility of implementing an Extended Kalman Filter (EKF).

4.2.1 Design

The design relies on a nonlinear model running in parallel to the plant. Both, plant and model are based on the same spatially discretized equations of the PDE (46) and are fed with the same inputs, namely the boundary conditions at $x = 0$, $x = L$ ($T_{Ammonia}$) and $y = 0$ (T_{Air}). The boundary conditions at $y = h$ are directly embedded in the spatially discretized equations of the plant and the model. The plant's equations look therefore as follows:

$$\begin{aligned} \dot{T} &= f_1(T), \\ y &= CT, \end{aligned} \tag{52}$$

where in fact $f_1(T)$ is given by equations in the form (51) with the respective difference expressions for distinct values for n and m. In order to introduce the design of the proposed EKF, we first introduce the standard Kalman-Bucy-Filter. Let the plant be in the form

$$\begin{aligned} \dot{x} &= f(x, u) + v, \\ y &= Cx + z, \end{aligned} \tag{53}$$

and thus the observer dynamics become

$$\begin{aligned} \dot{\hat{x}} &= A\hat{x} + Bu + KC(x - \hat{x}), \\ y &= Cx, \end{aligned} \tag{54}$$

where $A = \left.\frac{\partial f}{\partial x}\right|_{(x_0,u_0)}$ and $B = \left.\frac{\partial f}{\partial u}\right|_{(x_0,u_0)}$ are the Jacobians of $f(x, u)$ with respect to the state variables x and the input u, respectively, around an equilibrium point (x_0, u_0). C defines the output matrix and K is the observer feedback gain calculated by the Riccati differential equation

$$\dot{P} = AP + PA^T - PC^T R^{-1} CP + Q \tag{55a}$$

$$K = PC^T R^{-1}, \tag{55b}$$

where $Q = Q^T \geq 0$ and $R = R^T > 0$ denote the covariance matrices of the white Gaussian noise signals v representing errors in the model and z indicating measurement noise, respectively.

We propose the following observer dynamics for the EKF

$$\begin{aligned} \dot{\hat{T}} &= f_2(\hat{T}) + KC\left(T - \hat{T}\right) \\ y &= CT, \end{aligned} \tag{56}$$

where we use a nonlinear model for the observer, as can be seen by comparing (56) and (54). In (56), $f_2(\hat{T})$ is also given by equations in the form (51), just like $f_1(T)$. This means that A in the proposed design will only be used to calculate the solutions to the Riccati equation and thus to compute the observer feedback gain K.

4.2.2 Linearization

In contrast to the above mentioned standard design (54), the Jacobian in the proposed observer is not linearized around a fixed setpoint, but around the actual setpoints defined by the solutions to the ODEs, $\hat{T}_S$, meaning $A_{\hat{T}_S} = \left.\frac{\partial f_2}{\partial \hat{T}}\right|_{\hat{T}_S}$. Thus the system matrix $A_{\hat{T}_S}$ represents the linearized

system's behavior at particular points in state-space and changes as the system is progressing in time.

We define the state vector as

$$T = \begin{bmatrix} T_{1,1} & \cdots & T_{1,N} & T_{2,1} & \cdots & T_{2,N} & \cdots & T_{M,N} \end{bmatrix}^T,$$

and obtain a sparse matrix $A_{\hat{T}_S}$ with a regular pattern of diagonal and side-diagonal entries. Note that the system matrix can be subject to change due to the definition of the chosen parameter functions and also to the discretization scheme.

4.2.3 Measurements

It is assumed that no in-domain measurements are available, compare to Figure 4. Thus it is only possible to measure temperatures at the boundaries. This means that the output is

$$y = \begin{bmatrix} T_{1,1} & \cdots & T_{1,N} & T_{2,1} & T_{2,N} & \cdots & T_{M,1} & T_{M,N} \end{bmatrix}^T$$

which results in an output matrix on the following form

$$C = \text{blockdiag}\begin{bmatrix} C_1 & C_2 & \cdots & C_M \end{bmatrix}$$

where $C_1 = I_{(N\times N)}$ and $C_k = \begin{bmatrix} 1 & 0_{(1\times N-1)} \\ 0_{(1\times N-1)} & 1 \end{bmatrix}$ for $2 \leq k \leq M$.

4.2.4 Riccati equation

In this setup we use the matrix Riccati differential equation in the same form like (55)

$$\dot{P} = A_{\hat{T}_S} P + P A_{\hat{T}_S}^T - P C^T R^{-1} C P + Q \tag{57a}$$

$$K = P C^T R^{-1} \tag{57b}$$

where $Q = Q^T \geq 0$ and $R = R^T > 0$ represent the noise-covariance matrices of the signals v and z, respectively. We assume no correlation between single states and outputs. Note that the feedback gain K is actually a function of time and the linearization point $\hat{T}_S$.

The overall design can be seen in Fig. 5.

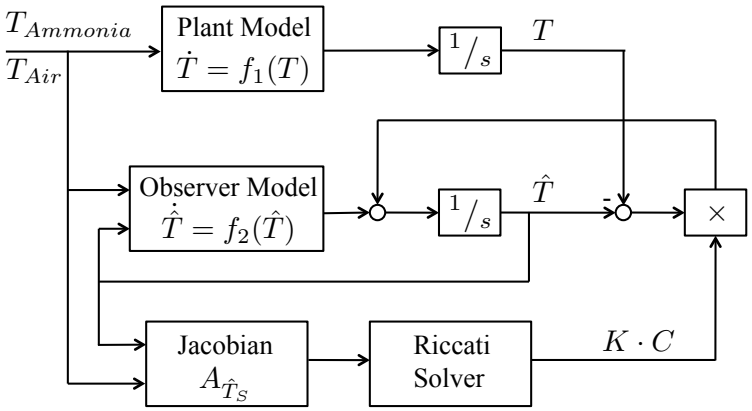

Figure 5. Design schematic

5. Simulation Examples

In this section simulation results for both the stability analysis and the observer design will be presented.

5.1 *Simulations regarding the stability analysis*

For the simulations we now return to the original freezing application, where we have chosen asymmetric boundary conditions and noisy initial conditions in order to exemplify the theoretical results in Section 3. Simulation parameters can be found in Backi and Gravdahl (2013) and represent a physical freezing process. Second order central differences and first order forward and central differences have been used to discretize the PDE (12) in its spatial coordinates only. This resulted in a set of coupled ODEs representing a spatial resolution of approximately 1×10^{-3} m ($N = 99$ discretization steps).

We present one case whose behavior has already been discussed in Backi, Bendtsen, Leth, and Gravdahl (2015).

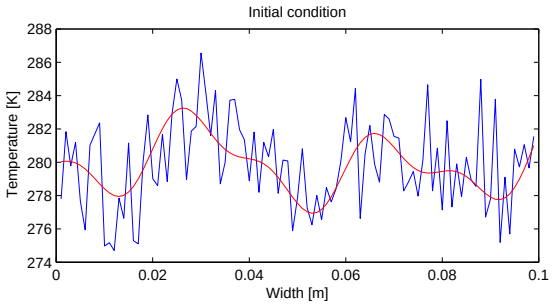

Figure 6. Initial condition, red: sum of sinusoidals, blue: sinusoidals plus added white Gaussian noise

Figure 6 shows the noisy initial condition that was chosen for the simulations. It consists of a sum of sinusoidals of different frequencies around $T = 280$ K plus added white Gaussian noise. The red line illustrates the sinusoidals alone whereas the blue line the overall noisy initial condition. By choosing the initial condition in this fashion we want to emphasize the damping character of the system.

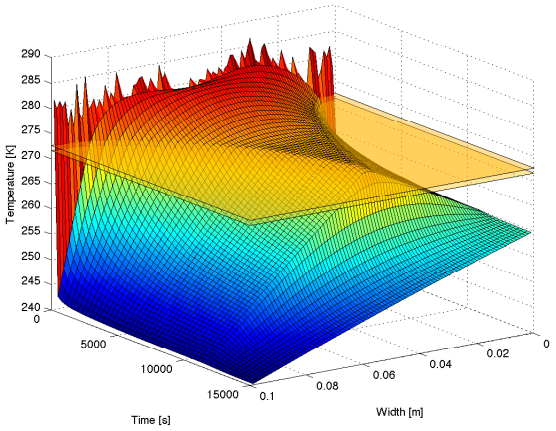

Figure 7. Asymmetric boundary conditions and noisy initial condition

In Figure 7 a simulation with boundary conditions $T(t, 0) = 260$ K and $T(t, 0.1) = 240$ K is presented. We can see that the temperature distribution converges towards the expected steady state

solution and is clearly stable in accordance with Theorem 1. Moreover, we can see the phenomenon of *thermal arrest*, which takes the form of a plateau of nearly constant temperatures inside $I_{\Delta T}$. The region $I_{\Delta T}$ is emphasized by the two orange planes. Furthermore, the *thermal arrest* is best visible in the very center of the spatial domain. The overall behavior corresponds with freezing curves obtained by measurements, as presented e.g. in Nicholson (1973).

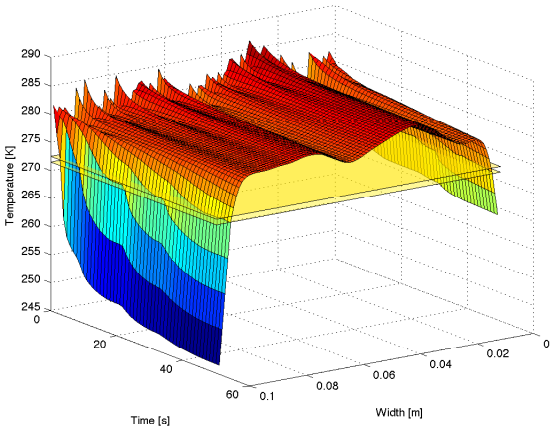

Figure 8. Asymmetric boundary conditions and noisy initial condition - 0 to 50 s

Figure 8 shows the behaviour in the first 50 s for the case shown in Figure 7. We do this in order to illustrate the converging and damping character even for noisy initial condition. As can be seen, the low-frequency parts of the sinusoidals are still present at the end of the simulation time, whereas the high-frequency peaks caused by white Gaussian noise get levelled out fairly fast.

5.2 *Simulations regarding the observer design*

The subsequent simulations have already been presented in Backi, Bendtsen, Leth, and Gravdahl (2014a). They have been conducted for a non-standard case, where white Gaussian noise was added to the measurements in order to investigate how the observer handles this phenomenon. The white noise was normed by its largest value, such that values between ± 1 K were added to the measurements. These values correspond to some degree with the specifications of measurement equipment, such as e.g. thermocouples[1]. Furthermore, to illustrate robustness, the parameters of the observer differ from those of the plant. In fact we chose the area of thermal arrest to be double the size for the observer, $\Delta T_{EKF} = 2\Delta T_{Sys}$, and the observers' parameter functions are 2 times larger than those of the system, meaning $k_{EKF} = 2k_{Sys}$ and $\kappa_{EKF} = 2\kappa_{Sys}$.

Simulation parameters can be found in the Appendix. The observer parameters were tuned by simulations and the initial conditions of the plant and the observer differ by 3 K. The values for N and M present a trade-off between accuracy and performance, as spatial resolution is limited by computational power. In addition, temperature variations along the y-coordinates for fixed x-positions are small, but not negligible. This justifies to choose M quite small, but greater than 1 ($M = 1$ represents a 1-dimensional PDE). Figure 9 shows plots for different x-coordinates at a fixed y-position (top layer of the fish block). The boundary layer can be seen in the top left, followed by the top right, bottom left and bottom right as we move along the x-axis towards the center of the domain. The center is shown in the plot in the bottom right. The area of thermal arrest is illustrated by the two gray areas (dark corresponds with ΔT_{EKF}, light with ΔT_{Sys}). The observer states are displayed in red, whereas the plant's states are shown in blue. The noisy measurement signal is illustrated in green.

[1]The standard EN 60584 defines three accuracy classes, where the first allows deviations of ± 1.5 K

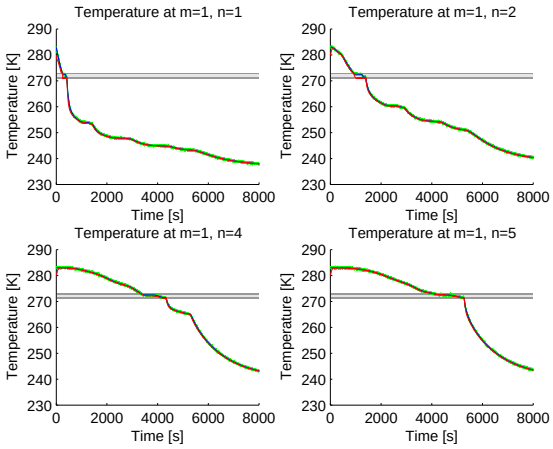

Figure 9. Observer states (red), real states (blue) and noisy measurement signals (green) at $m = 1$ and $n = 1, 2, 4, 5$

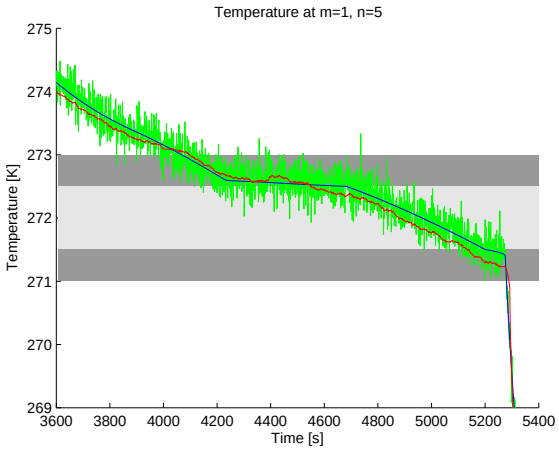

Figure 10. Zoom of observer state (red), real state (blue) and noisy measurement signal (green) at $m = 1$ and $n = 5$

In Figure 10 a zoom into the bottom right plot in Figure 9 is illustrated. Due to the fact that the state can be measured, the observer state is following the real state quite accurately, even in the presence of white Gaussian noise.

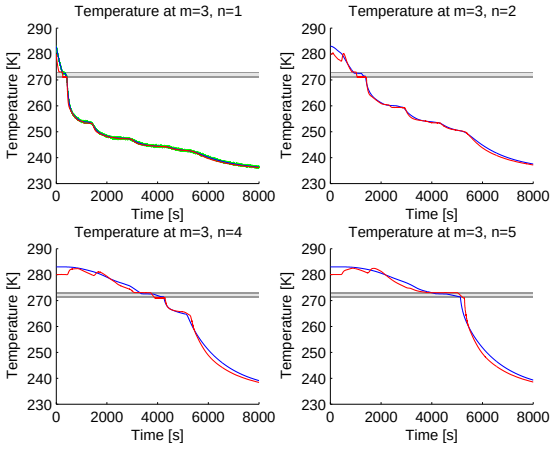

Figure 11. Observer states (red), real states (blue) and noisy measurement signals (green) at $m = 3$ and $n = 1, 2, 4, 5$

Figure 11 presents plots for different x-coordinates at the center of the y-coordinate ($m = 3$). Only the top left plot includes the noisy measurement signal, as it is the only measurable state in the set of illustrated states. As can be seen the observer follows the real states quite satisfyingly.

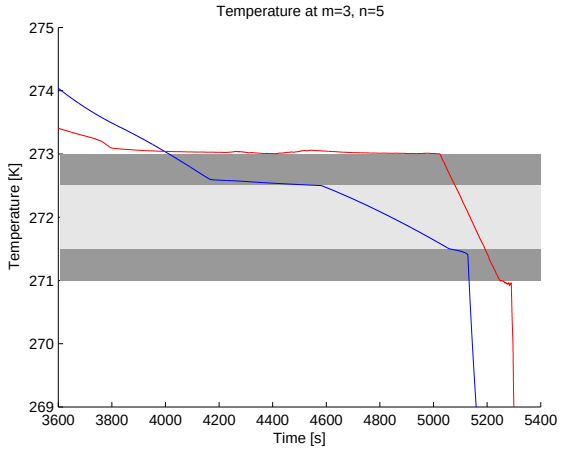

Figure 12. Zoom of observer state (red) and real state (blue) at $m = 3$ and $n = 5$

Figure 12 shows a zoom into the bottom right plot in Figure 11. Comparing this to Figure 10, one can see that now in the absence of measurement, the observer doesn't follow the real state as accurately.

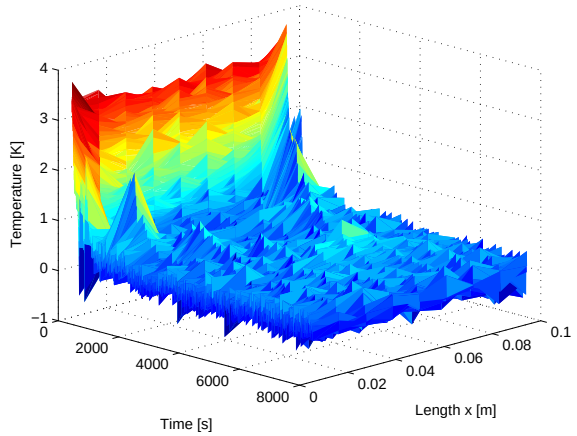

Figure 13. Observer error at $m = 1$

In Figures 13 and 14 the error between real and observed state is shown along the x-coordinate for a fixed y-position (top and bottom of the block, respectively). It can be seen that the error is brought back to zero for both cases, even in the presence of noisy measurements and diverging parameters.

6. Conclusions

In this paper we presented a stability investigation for a partial differential equation with state-dependent parameter functions and asymmetric boundary conditions. The PDE is a heat equation derived from the diffusion equation. The work originates in a freezing application and presents a generalization to already established stability results for the same heat equation with symmetric

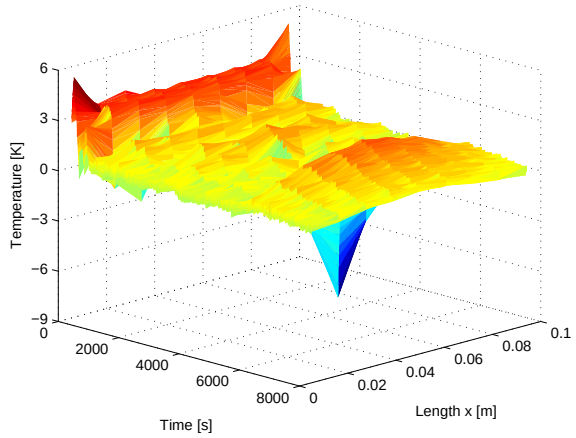

Figure 14. Observer error at $m = 5$

boundary conditions. Numerical simulations indicate that the theoretical results do in fact hold for the freezing application. As pointed out in Backi, Bendtsen, Leth, and Gravdahl (2014b) we firstly proved stability in the sense of convergence in both L^2- and H^1-norms, and secondly in terms of absolute value of the solution's transient part. The conservativeness of the restrictions on derivatives and signs of the coefficient functions can be relaxed in practice as shown by the simulations.

Furthermore, we presented an observer design for the aforementioned PDE. The observer is based upon an Extended Kalman Filter (EKF) with the purpose of estimating the temperature distribution inside the spatial domain. The results presented show that the non-measurable states in the inner domain are estimated quite accurately, even in the case of uncertain parameter functions. In addition, the presence of white Gaussian noise in the measurement signals is handled well by the observer. Thus it can be concluded that the design is robust to parameter variations and noise.

References

Backi, C. J., Bendtsen, J. D., Leth, J., & Gravdahl, J. T. (2014a). Estimation of inner-domain temperatures for a freezing process. In *Proceedings of the 2014 ieee multi-conference on systems and control.* Antibes, France.

Backi, C. J., Bendtsen, J. D., Leth, J., & Gravdahl, J. T. (2014b). The nonlinear heat equation with state-dependent parameters and its connection to the burgers' and the potential burgers' equation. In *Proceedings of the 19th ifac world congress.* Cape Town, South Africa.

Backi, C. J., Bendtsen, J. D., Leth, J., & Gravdahl, J. T. (2015). Stability properties of a heat equation with state-dependent parameters and asymmetric boundary conditions. In *Proceedings of the 1st conference on modelling, identification and control of nonlinear systems (micnon).* Saint Petersburg, Russia.

Backi, C. J., & Gravdahl, J. T. (2013). Optimal boundary control for the heat equation with application to freezing with phase change. In *Proceedings of the 3rd australian control conference.* Perth, Australia.

Balogh, A., & Krstic, M. (2000). Burgers' equation with nonlinear boundary feedback: H1 stability, well–posedness and simulation. *Mathematical Problems in Engineering*, *6*, 189–200.

Çengel, Y. A., & Boles, M. A. (2004). *Thermodynamics - an engineering approach* (5th, Ed.). McGraw-Hill Science/Engineering/Math.

Cleland, D. J., Cleland, A. C., & Earle, R. L. (1987). Prediction of freezing and thawing times for multi-dimensional shapes by numerical methods. *International Journal of Refrigeration*, *10*, 32–39.

Cleland, D. J., Cleland, A. C., Earle, R. L., & Byrne, S. J. (1987, January). Experimental data for freezing and thawing of multi-dimensional objects. *International Journal of Refrigeration*, *10*, 22–31.

Cole, J. D. (1951). On a quasi-linear parabolic equation occuring in aerodynamics. *Quarterly of Applied Mathematics*, *9*, 225–236.

Costa, M., Buddhi, D., & Oliva, A. (1997). Numerical simulation of a latent heat thermal energy storage system with enhanced heat conduction. *Energy Conversion and Management*, *39*(3/4), 319–330.

Hasan, A., Sagatun, S., & Foss, B. (2010). Well rate control design for gas coning problems. In *Proceedings of the 49th ieee conference on decision and control* (pp. 5845–5850). Atlanta, GA, USA.

Henry, D. (1981). *Geometric theory of semilinear parabolic equations* (Vol. 840). Berlin: Springer-Verlag.

Heredero, R. H., Levi, D., & Winternitz, P. (1999). Symmetries of the discrete burgers equation. *Journal of Physics A: Mathematical and General*, *32*(14), 2685-2695.

Hidayat, Z., Babuska, R., Schutter, B. D., & Nunez, A. (2011). Observers for linear distributed-parameter systems: A review. In *Proceedings of the 2011 ieee international symposium on robotic and sensors environment (rose)*. Montreal, Canada.

Hills, R. G. (2006). Model validation: Model parameter and measurement uncertainty. *Journal of Heat Transfer*, *128*(4), 339–351.

Hopf, E. (1950, September). The partial differential equation ut + uux = μuxx. *Communications on Pure and Applied Mathematics*, *3*(3), 201–230.

Kobayashi, T., & Hitotsuya, S. (1981). Observers and parameter determination fir distributed parameter systems. *International Journal of Control*, *33*(1), 31–50.

Korshunova, A. A., & Rozanova, O. S. (2009). The riemann problem for the stochastically perturbed non-viscous burgers equation and the pressureless gas dynamics model. In *Proceedings of the international conference days on diffraction, dd 2009* (pp. 108–113). St. Petersburg, Russia.

Krstic, M. (1999). On global stabilization of burgers' equation by boundary control. *Systems & Control Letters*(37), 123–141.

Krstic, M., Magnis, L., & Vazquez, R. (2008, August). Nonlinear stabilization of shock-like unstable equlibria in the viscous burgers pde. *IEEE Transactions on Automatic Control*, *53*(7), 1678–1683.

Krstic, M., Magnis, L., & Vazquez, R. (2009, March). Nonlinear control of the viscous burgers equation: Trajectory generation, tracking and observer design. *Journal of Dynamic Systems, Measurement and Control*, *131*.

Krstic, M., & Smyshlyaev, A. (2008). *Boundary control of pdes - a course on backstepping.* Society for Industrial and Applied Mathematics.

Muhieddine, M., Canot, É., & March, R. (2008). Various approaches for solving problems in heat conduction with phase change. *International Journal of Finite Volume Method*, *6*(1).

Nicholson, F. J. (1973). *The freezing time of fish* (Tech. Rep. No. 62). Torry Research Station.

Pham, Q. T. (1984). Extension to planck's equation for predicting freezing times of foodstuffs of simple shapes. *International Journal of Refrigeration*, *7*(6), 377–383.

Pham, Q. T. (1985a). Analytical method for predicting freezing times of rectangular blocks of foodstuffs. *International Journal of Refrigeration*, *8*(1), 43–47.

Pham, Q. T. (1985b). A fast, unconditionally stable finite-difference scheme for heat conduction with phase change. *International Journal of Heat and Mass Transfer*, *28*, 2079–2085.

Pham, Q. T. (2006a). Mathematical modeling of freezing processes. In *Handbook of frozen food processing and packaging* (chap. 7). Taylor & Francis Group, LLC.

Pham, Q. T. (2006b). Modelling heat and mass transfer in frozen foods: a review. *International Journal of Refrigeration*, *29*, 876–888.

Plank, R. (1941). Beiträge zur Berechnung und Bewertung der Gefriergeschwindigkeit von Lebensmitteln. *Zeitschrift für die gesamte Kälte-Industrie*(10).

Prüss, J., Saal, J., & Simonett, G. (2007). Existence of analytic solutions for the classical stefan problem. *Mathema-tische Annalen*, *338*, 703–755.

Sallberg, S. A., Maybeck, P. S., & Oxley, M. E. (2010). Infinite-dimensional sampled-data kalman filtering and the stochastic heat equation. In *Proceedings of the 49th ieee conference on decision and control.* Atlanta, GA, USA.

Smyshlyaev, A., & Krstic, M. (2010). *Adaptive control of parabolic pdes.* Princeton, New Jersey, USA: Princeton University Press.

Sophocleous, C. (2004). Transformation properties of a variable-coefficient burgers equation. *Chaos, Solitons and Fractals*, *20*(5), 1047–1057.

Sugimoto, N., & Kakutani, T. (1985). 'generalized burgers' equation' for nonlinear viscoelastic waves. *Wave Motion*, *7*(5), 447–458.

Woinet, B., Andrieu, J., & Laurent, M. (1998). Experimental and theoretical study of model food freezing. part 1. heat transfer modelling. *Journal of Food Engineering*, *35*, 381–393.